Electronic Supplementary Material (ESI) for Materials Advances.

Supporting information

A Low-Cost and Li-Rich Organic Coating on $Li_4Ti_5O_{12}$ Anode Material Enabling Li-Ion Battery Cycling at Subzero Temperatures

Nicolas Delaporte[1], Pascale Chevallier[2], Sylviane Rochon[1], Gilles Lajoie[1], Jean-Christophe Daigle[1], Vincent Gariepy[1], René Veillette[1], Marie-Claude Mathieu[1], Manon Provencher[1], Michel L. Trudeau[1], Karim Zaghib[1]*

1. Center of Excellence in Transportation, Electrification and Energy Storage, 1806 Bd. Lionel-Boulet, Varennes, QC, Canada.
2. Research center of the CHU de Québec – Laval University, St François d'Assise, 10 Espinay St., Quebec city, QC, Canada.

Corresponding author:
*Zaghib.Karim@hydro.qc.ca

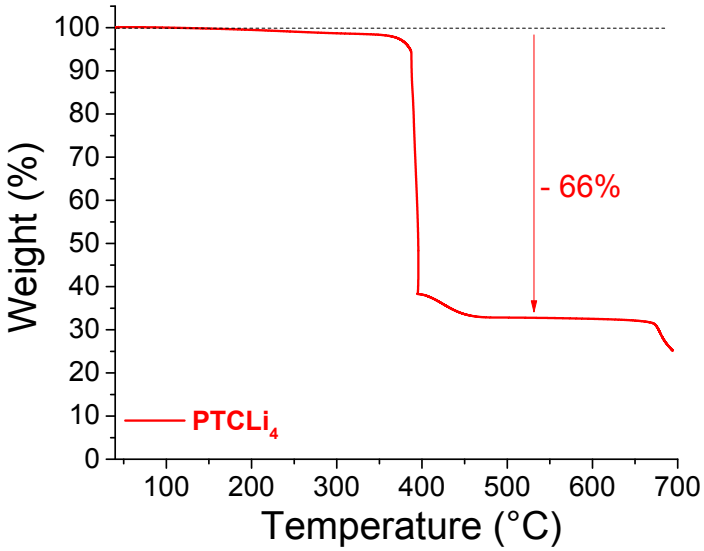

Figure SI1. Thermogravimetric curve under air flow for $PTCLi_4$ powder.

To confirm the coverage of LTO with $PTCLi_4$, SEM analyses are performed and optical images of bare LTO and LTO@2%$PTCLi_4$ powders are shown in Figure SI2a. The pristine LTO powder was composed of primary particles of nanometer size forming large secondary spherical aggregates of a few micrometers to 20–30 µm in diameter. Many voids form between the primary particles of the LTO powder. In contrast, it is clearly seen that for the LTO@2%$PTCLi_4$ sample, most of the voids are filled with the organic molecules, as indicated with red arrows in Figure SI2a. Furthermore, note that large crystalline $PTCLi_4$ particles (see Figure 1c in the manuscript) are not observed in the composite powder, which further confirms the coverage of LTO with $PTCLi_4$ rather than a mixture of these two materials. In addition, the EDX profile for $PTCLi_4$-coated LTO powder presented in Figure SI2b shows the presence of carbon in addition to high amounts of oxygen and titanium from the LTO particles. The elemental mappings of oxygen, titanium, and carbon for a small surface area of the modified powder reveal that carbon was present everywhere

on the surface of the anode material and that the voids are effectively rich in carbon (i.e., $PTCLi_4$) as indicated by red/white circles in Figure SI2c.

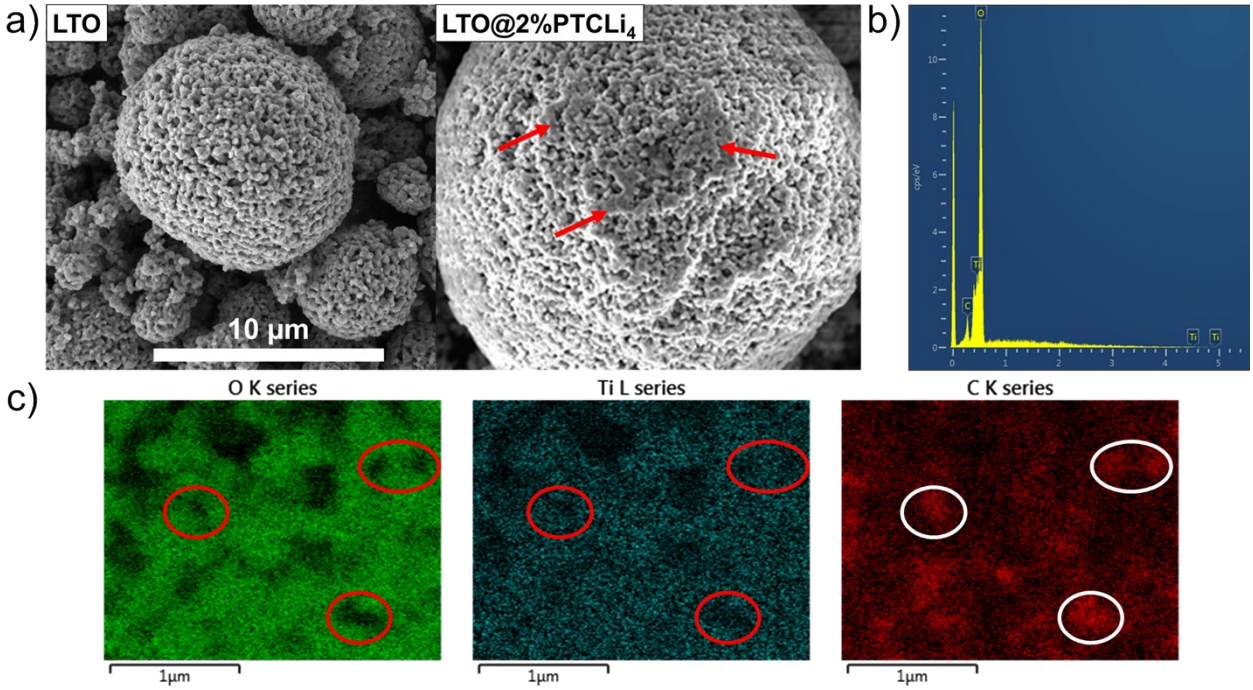

Figure SI2. a) SEM images of LTO and LTO@2% $PTCLi_4$ powders. b) Energy-dispersive X-ray (EDX) spectroscopy profile and c) elemental mappings of O (green), Ti (blue), and C (red) for LTO@2% $PTCLi_4$ sample.

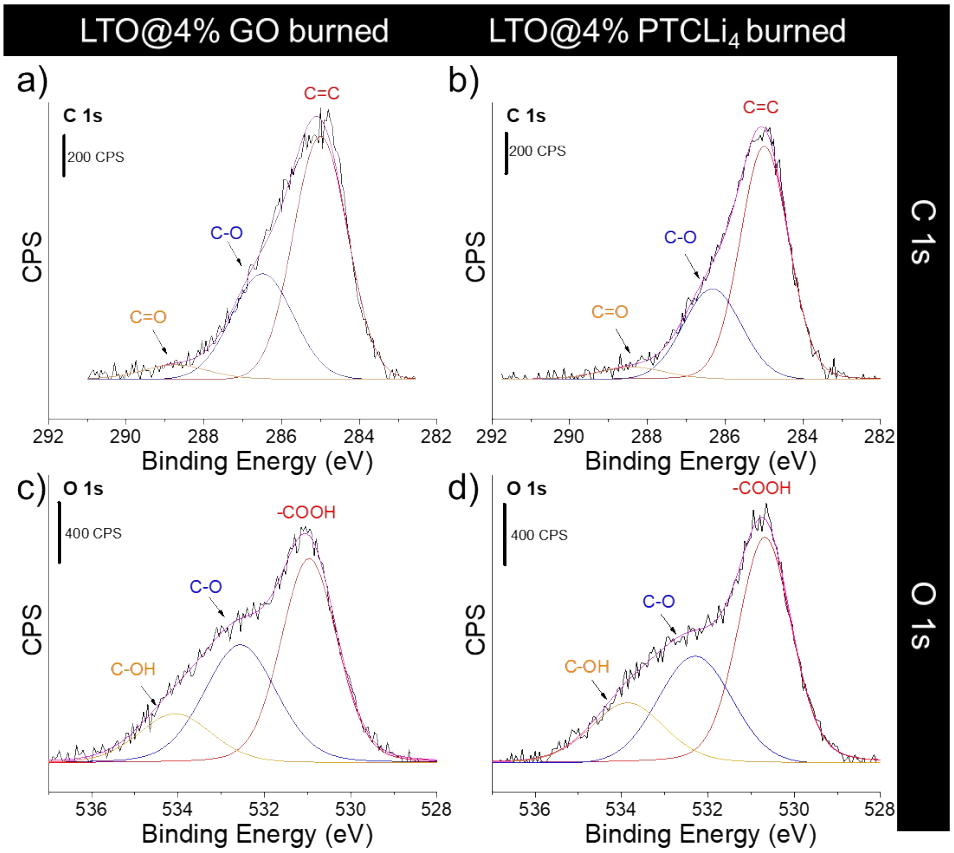

Figure SI3. XPS a,b) C 1s and c,d) O 1s core level spectra for a,c) LTO@4% GO burned and b,d) LTO@4% $PTCLi_4$ burned powders.

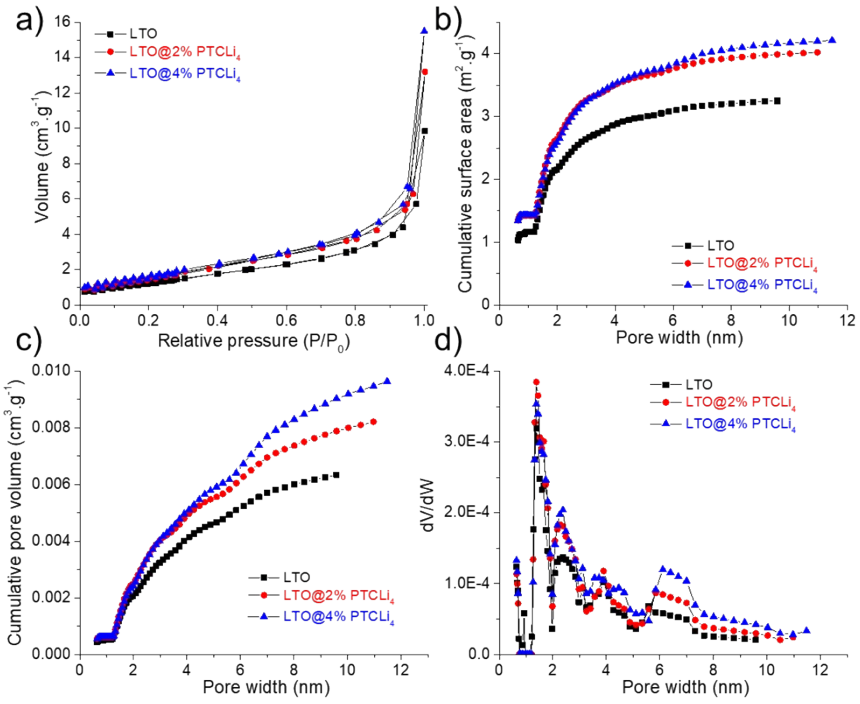

Figure SI4. a) Nitrogen adsorption–desorption isotherms at 77 K, b) cumulative surface area vs. pore width, c) cumulative volume vs. pore width, and d) pore size distribution (dV/dW) for LTO (■), LTO@2% $PTCLi_4$ (●) and LTO@4% $PTCLi_4$ (▲).

Table SI1. Specific surface areas for LTO, LTO@2% $PTCLi_4$, and LTO@4% $PTCLi_4$ powders.

Sample	**LTO**	**LTO@2% $PTCLi_4$**	**LTO@4% $PTCLi_4$**
BET surface area ($m^2 \cdot g^{-1}$)	4.7	5.9	6.3

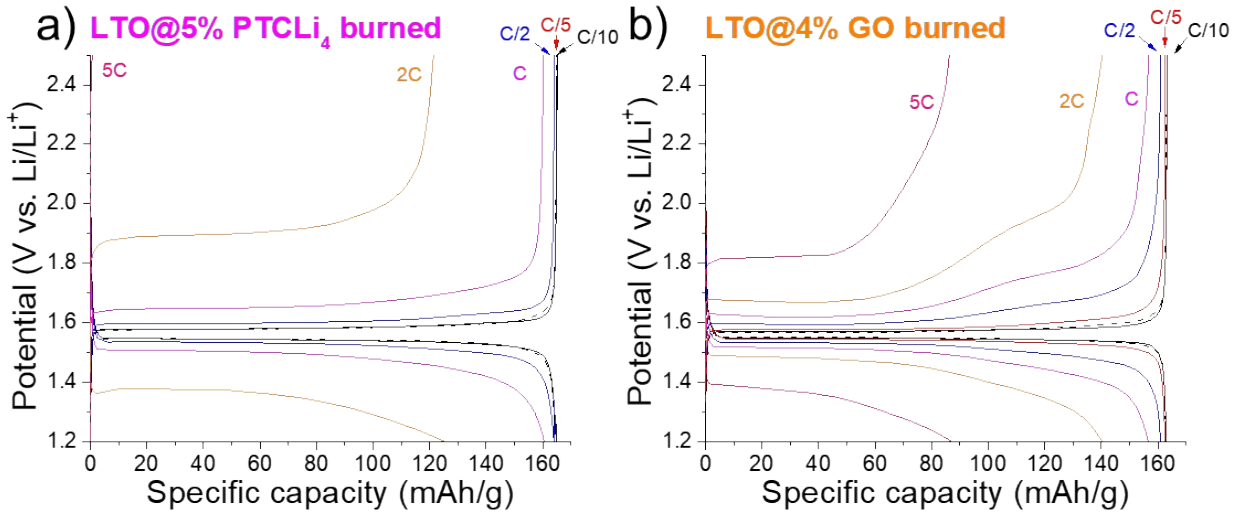

Figure SI5. Galvanostatic charge/discharge profiles at different cycling rates for a) LTO@5% $PTCLi_4$ burned and b) LTO@4% GO burned electrodes. First cycle at C/10 (– – –) and fifth cycle for each cycling rate are represented.